ApoA-I Milano stimulates lipolysis in adipose cells independently of cAMP/PKA activation[s]

Maria Lindahl,*,[†] Jitka Petrlova,* Jonathan Dalla-Riva,* Sebastian Wasserstrom,[†] Catarina Rippe,§ Joan Domingo-Espin,* Dorota Kotowska,[†] Ewa Krupinska,* Christine Berggreen,** Helena A. Jones,[††] Karl Swärd,§ Jens O. Lagerstedt,* Olga Göransson,** and Karin G. Stenkula[1],[†]

Medical Protein Science,* Glucose Transport and Protein Trafficking,[†] Cellular Biomechanics,§ Protein Phosphorylation,** and Molecular Endocrinology,[††] Department of Experimental Medical Science, Biomedical Center, Lund University, 221 84 Lund, Sweden

Abstract ApoA-I, the main protein component of HDL, is suggested to be involved in metabolic homeostasis. We examined the effects of Milano, a naturally occurring ApoA-I variant, about which little mechanistic information is available. Remarkably, high-fat-fed mice treated with Milano displayed a rapid weight loss greater than ApoA-I WT treated mice, and a significantly reduced adipose tissue mass, without an inflammatory response. Further, lipolysis in adipose cells isolated from mice treated with either WT or Milano was increased. In primary rat adipose cells, Milano stimulated cholesterol efflux and increased glycerol release, independently of β-adrenergic stimulation and phosphorylation of hormone sensitive lipase (Ser563) and perilipin (Ser522). Stimulation with Milano had a significantly greater effect on glycerol release compared with WT but similar effect on cholesterol efflux. Pharmacological inhibition or siRNA silencing of ABCA1 did not diminish Milano-stimulated lipolysis, although binding to the cell surface was decreased, as analyzed by fluorescence microscopy. Interestingly, methyl-β-cyclodextrin, a well-described cholesterol acceptor, dose-dependently stimulated lipolysis.⬛ Together, these results suggest that decreased fat mass and increased lipolysis following Milano treatment in vivo is partly explained by a novel mechanism at the adipose cell level comprising stimulation of lipolysis independently of the canonical cAMP/protein kinase A signaling pathway.—Lindahl, M., J. Petrlova, J. Dalla-Riva, S. Wasserstrom, C. Rippe, J. Domingo-Espin, D. Kotowska, E. Krupinska, C. Berggreen, H. A. Jones, K. Swärd, J. O. Lagerstedt, O. Göransson, and K. G. Stenkula. **ApoA-I Milano stimulates lipolysis in adipose cells independently of cAMP/PKA activation.** *J. Lipid Res.* 2015. 56: 2248–2259.

Supplementary key words adipose tissue • apolipoprotein A-I • cholesterol • diabetes • obesity • adenosine 3′,5′-cyclic monophosphate • protein kinase A

HDL is well known for its protective role in vascular wall function through regulation of reversed cholesterol transport (1, 2). In addition, beneficial effects of HDL and its main protein component, ApoA-I, on glucose homeostasis have recently been reported, and both type 2 diabetes and insulin resistance are associated with reduced plasma concentrations of HDL (3, 4). Moreover, HDL infusion in type 2 diabetes subjects increased both insulin secretion and glucose clearance (5). Besides effects on glucose homeostasis, several animal studies have shown that increased ApoA-I/HDL levels are associated with reduced body weight and improved insulin sensitivity (6, 7). In recent studies, ApoA-I-deficient (ApoA-I$^{-/-}$) mice showed increased body weight and fat mass and less propensity for weight loss during calorie restriction, in part explained by reduced lipolysis (8, 9).

Fully differentiated adipose cells contain a large amount of nonesterified cholesterol located in the lipid droplet. With increasing cell size, the lipid droplet-associated cholesterol pool increases further by redistribution of cholesterol from the plasma membrane pool (10). This rearrangement could contribute to adipose cell dysfunction associated with obesity (11), one of the main risk factors for insulin resistance and metabolic diseases including type 2 diabetes and cardiovascular complications (12). Despite the large cholesterol pool, there is a limited de novo cholesterol synthesis in adipose cells (10). Instead, extracellular cholesterol is internalized through different pathways, including CD36 (13), scavenger receptor class B type I (14), and LDL receptor-related protein in conjunction with apoE (15). Cholesterol efflux from adipose cells to

This article is available online at http://www.jlr.org

HDL is mediated through ABCA1 (16), but most likely also involves ABCG1 and other still unknown pathways (17). Many studies have focused on the role of caveolae for cholesterol efflux, with conflicting results (18, 19). Le Lay et al. (18) proposed that interaction of ApoA-I with caveolin-1, the main structural caveolar protein, could occur without promoting cholesterol efflux, which supports alternative, caveolae-independent pathways. In contrast, Sviridov et al. (19) suggested that ApoA-I regulates both caveolin-1 expression and intracellular cholesterol trafficking to caveolae. Of interest, evidence suggests that β-adrenergic stimulated lipolysis increases cholesterol efflux, emphasizing a balance between triglyceride and cholesterol storage (20, 21).

Together, considerable information is available about the systemic and the cellular effects of ApoA-I WT. However, there is less knowledge regarding the naturally occurring ApoA-I Milano variant, which contains a single point mutation that leads to an Arg(173)Cys substitution. Humans carrying the Milano variant have lowered HDL and increased circulating triglyceride levels, without increased risk for cardiovascular diseases (22). The beneficial properties of ApoA-I Milano have been suggested to be due to its efficiency in mediating cholesterol efflux and its potential to suppress inflammation (23). We have recently reported that acute treatment of insulin-resistant, diet-induced obese mice with recombinant Milano increases plasma glucose clearance and improves insulin secretion to the same extent as ApoA-I WT (24). Thus, we decided to further characterize the effects of ApoA-I Milano in vivo and in vitro. Here, we report that injections of ApoA-I in insulin-resistant mice induce rapid weight loss and increase lipolysis without triggering an inflammatory response. The effect on lipolysis was verified in isolated rat adipose cells, in which both ApoA-I WT and Milano induced lipolysis, independent of cAMP/protein kinase A (PKA) and activation of hormone sensitive lipase (HSL). Surprisingly, the Milano-stimulated effect was much greater compared with both ApoA-I WT and β-adrenergic stimulated lipolysis. We report that Milano triggered cholesterol efflux in both primary adipose cells and 3T3-L1 adipose cells, and we provide data that suggest that ABCA1 is not required to mediate these effects. The results propose a novel, but complex relationship at the cellular level between cholesterol efflux, a redistribution of the intracellular cholesterol and triglyceride pools, and regulation of lipolysis independently of the canonical cAMP/PKA signaling pathway.

METHODS

Reagents

Anti-HSL pSer563, anti-HSL pSer565 antibodies (Cell Signaling Technologies) and anti-HSL antibodies were kindly provided by Cecilia Holm (Lund University, Sweden); anti-perilipin and anti-perilipin pSer522 antibodies were from Valia Science; anti-adipose triglyceride lipase, anti-ABCA1, and anti-ApoA-I antibodies were from Abcam; anti-caveolin-1 and -2, anti-pPKA consensus antibodies were obtained from Cell Signaling Technologies; and anti-actin antibodies were from Sigma. Anti-pSIK2 Ser358 antibodies were generated in house as described previously (25), orlistat was from Sigma, and D-^{14}C(U)-glucose was from Perkin Elmer.

Production of recombinant ApoA-I protein

A bacterial expression system consisting of pNFXex plasmid in *Escherichia coli* strain BL21(DE3) pLysS cells (Invitrogen) was used to generate the ApoA-I proteins as previously described (26, 27). Primer-directed PCR mutagenesis was used to create the Arg(173)Cys substitution, and the mutation was verified by dideoxy-automated fluorescent sequencing. After protein purification, tobacco etch virus protease was used to cleave off the His tag used for purification using a Ni column. The samples were desalted into phosphate buffered saline, pH 7.4, 150 mM NaCl, concentrated with 10 kDa molecular mass cutoff Amicon Ultra centrifugal filter devices (Millipore), and stored at 4°C prior to use. Protein purity was confirmed by SDS-PAGE with Coomassie blue staining and concentrations determined by Nanodrop, using molecular mass and extinction coefficient.

ApoA-I injection of C57BL/6J mice

C57BL/6J mice (Taconic), 10- to 12-week-old males, fed a high-fat diet (HFD) for 2 weeks (24), were injected intraperitoneally with either ApoA-I WT or ApoA-I Milano (20 mg/kg in phosphate-buffered saline, pH 7.4; control animals received NaCl) once daily for 6 days. Twenty-four hours after the last treatment, blood was sampled through vena saphena; blood glucose levels were measured using OneTouch Ultra2 (Lifescan); white blood cell (WBC) count was measured using a semiautomatic cell counter SYSMEX KX-21N; and insulin levels, cytokines, and FFAs (NEFAs) were assayed in serum. Adipose tissue was collected for Western blot analysis. The local animal ethics committee in Lund/Malmö approved all experiments.

Insulin assay

Serum samples were analyzed for insulin using a mouse insulin ELISA (10-1247-01; Mercodia AB, Uppsala, Sweden). All samples were analyzed in duplicate with a sample volume of 5 µl according to the supplier's instructions.

NEFAs

Serum samples were analyzed for NEFAs using a NEFA-HR (2) kit (Wako Chemicals GmbH, Neuss, Germany). All samples were analyzed in duplicate with a sample volume of 3.5 µl according to the supplier's instructions.

Cytokine analysis

Serum samples collected 24 h after injections were analyzed for TNF-α and interleukin 6 (IL-6) by an LSRII flow cytometer assay (BD Biosciences) (28). Serum samples collected after completed treatment (day 7) were analyzed for TNF-α, IL-6, and IFN-γ using an MSD Multi-Spot assay system Proinflammatory Panel 1 (mouse) kit. All samples were analyzed in duplicate according to the supplier's instructions.

Dual-energy X-ray absorptiometry

To determine the percentage of body fat, the mice were placed in a dual-energy X-ray absorptiometry (DEXA) scanner (PixiMouse, GE Healthcare), and body composition was measured.

Isolation and stimulation of primary adipose cells

Rat adipose cells were isolated from 36- to 40-day-old male Sprague Dawley rats, as described previously (29). The cells were suspended (10% suspension) in Krebs-Ringer (KRH) medium

containing 25 mM HEPES pH 7.4, 200 nM adenosine, 2 mM glucose, and 1% BSA (w/v) and stimulated as indicated in the figures. To stop incubations, cells were washed in KRH without BSA and subsequently lysed in a buffer containing 50 mM Tris/HCl pH 7.5, 1 mM EGTA, 1 mM EDTA, 1 mM sodium orthovanadate, 10 mM sodium-β-glycerophosphate, 50 mM sodium fluoride, 5 mM sodium pyrophosphate, 0.27 M sucrose, 1% NP-40, 1 mM DTT, and complete protease inhibitor cocktail (1 tablet/50 ml) (lysis buffer). Lysates were centrifuged for 15 min at 13,000 g, 4°C, and protein concentrations were determined by Bradford. To obtain the lipid droplet fraction, the fat cakes following centrifugation were processed according to previously described method (30). Briefly, the fraction was recentrifuged, warmed to room temperature, and vortexed with SDS sample buffer. The sample was centrifuged for 15 min at 13,000 g, 4°C, and protein was extracted from the lipid droplet collected from beneath the fat layer. Mouse adipose cells from epididymal adipose tissue of caveolin-1 KO or C57BL/6J WT mice were isolated as described above, with KRH buffer containing 3% BSA. For adipose tissue lysates, intact tissue was homogenized with a polytron (Omni International TH) in lysis buffer and treated as above.

Lipolysis assay

To measure lipolysis, rat or mouse adipose cells [400 µl of a 5% (v/v) suspension] were suspended in KRH medium and treated with ApoA-I or isoproterenol as indicated in the figures (at 37°C, with shaking, 150 cycles/min). After 30 min, samples were placed on ice for 20 min, and 200 µl of the cell medium was subsequently removed for enzymatic determination of the glycerol content, as described previously (31). The cells were washed twice with KRH medium without BSA and lysed in lysis buffer as described above.

Western blot

Cell lysates (10 µg total protein) were heated at 95°C for 2 min in lithium dodecyl sulfate sample buffer, and subjected to PAGE on precast BioRad gradient gels and electrotransfer to nitrocellulose membrane. Membranes were blocked for 30 min in 50 mM Tris/HCl pH 7.6, 137 mM NaCl, and 0.1% (w/v) Tween-20 (TBS-T) containing 10% (w/v) milk. The membranes were then probed with indicated antibodies in TBS-T containing 5% (w/v) milk or 5% (w/v) BSA, for 16 h at 4°C. Detection was performed using horseradish peroxidase-conjugated secondary antibodies and the enhanced chemiluminescence reagent. The signal was visualized using a LI-COR Image camera, and band intensities were quantified using Licor Imaging software (Licor).

Culture and differentiation of 3T3-L1 adipose cells

3T3-L1 fibroblasts were cultured at subconfluence in DMEM medium containing 10% FCS (v/v) and 1% penicillin/streptomycin (v/v) at 5% CO_2 in 37°C. Two days postconfluence (designated as day 0), cells were incubated with DMEM medium containing 10% FCS (v/v) and 1% penicillin/streptomycin (v/v) supplemented with 0.5 mM 3-isobutyl-1-methylxanthine, 10 µg/ml insulin, and 1 µM dexamethasone for 48 h. After that, the medium was changed to DMEM supplemented with 10 µg/ml insulin for 48 h, cells were hereafter cultured in DMEM medium containing 10% FCS (v/v) and 1% penicillin/streptomycin (v/v), and culture medium was changed every second day. Experiments were performed on days 8–11 after the initiation of differentiation (day 0), at which differentiation rate was typically 80–90%.

siRNA silencing

Mature 3T3-L1 adipose cells (8–9 days post differentiation) were transfected with siRNA by electroporation as described previously (32). Three siRNAs targeting ABCA1 (sense: GGGU-GGACGAGUUUCGGUAtt, antisense: UACCGAAACUCGUU-CACCCAg; sense: GGAACGGGUUACUAUCUGAtt, antisense: UCAGAUAGUAACCCGUUCCca; sense: CGAGGAUAACAACU-ACAAAtt, antisense: UUUGUAGUUGUUAUCCUCGta), and Silencer® Select Negative Control No. 1 (cat number 4390844) were purchased from Ambion® and were used at final concentration of 0.5 nM each (1.5 nM total) on mature adipose cells (days 8–9). Forty-eight hours after electroporation, cells were stimulated with ApoA-I Milano (150 µg/ml), ApoA-I WT (150 µg/ml), isoproterenol (100 nM), or PBS for 2 h. After that, medium was collected for glycerol determination, and total RNA was collected using QIAzol™ reagent (Qiagen).

RNA preparation and quantitative real-time PCR

Analysis of gene expression in 3T3-L1 mature adipose cells transfected with ABCA1 siRNA and treated with ApoA-I Milano, ApoA-I WT, isoproterenol, or PBS was assessed by quantitative real-time PCR. Cells were lysed and homogenized in Qiazol™ lysis reagent, and total RNA was isolated using RNeasy® Mini Kit (Qiagen) according to the manufacturer's recommendations. Total RNA (1 µg) was treated with DNase I (Invitrogen) enzyme and reverse transcribed using random hexamers (Invitrogen) and SuperScript™II (Invitrogen) RNaseH reverse transcriptase according to the manufacturer's recommendations. The cDNA was used in quantitative PCR reactions using TaqMan chemistry (Applied Biosystems) in an ABI 7900 Sequence Detection System. Relative abundance of mRNA was calculated using geometric averaging of TBP and Rps29 control genes.

Cholesterol efflux

3T3-L1 adipocytes (days 7–12 of differentiation) cultured in 10 cm plates were harvested by trypsin/collagenase (type 1, Gibco 17100-017, final concentration 1 mg/ml) digestion and then reseeded into 24-well plates. One day postseeding, cells were rinsed twice with PBS and then loaded with labeled cholesterol by culturing in DMEM containing 5% FBS, P/S, and 4 µCi/ml ^{3}H-cholesterol (Perkin Elmer #NET139001MC, specific activity 19 Ci/mmol) for 24 h. To maximize the availability of free cholesterol for efflux, 2 µg/ml of an inhibitor of ACAT (Sandoz58-035, Sigma) was also included. Subsequently, cells were rinsed twice with PBS and cultured for another 18 h in DMEM containing 0.2% BSA, P/S, and 2 µg/ml of the ACAT inhibitor, to enable equilibration of cellular cholesterol pools. Finally, cells were rinsed twice with PBS and then treated with ApoA-1 WT or Milano (or PBS as a control) at indicated concentrations for 3 h. Medium was collected and centrifuged at 14,000 g for 5 min to remove any floating cells, and the amount of labeled cholesterol was measured by scintillation counting. To normalize for potential differences in the amount of cholesterol loaded, cells were lysed and scraped in 0.1 M NaOH, a portion of the cell lysate was counted, and cholesterol efflux was expressed as cholesterol in the medium/(cholesterol in the medium + cholesterol in cell lysates).

Isolated primary rat adipose cells were incubated with a BODIPY-cholesterol solution in MEM [0.05 mM BODIPY-cholesterol "Topfluor" (Avantipolar lipids)], 0.2 mM unlabeled cholesterol, and 10 mM methyl-B-cyclodextrin (mβCD), prepared according to (33) for 1 h at 37°C. The ratio of cells to BODIPY-cholesterol solution was 1:2 (v/v), with a final concentration of 1% BSA (w/v) and 200 nM adenosine. Cells were then washed three times with KRH medium without glucose and equilibrated for 1 h at 37°C. Uptake of BODIPY-cholesterol into adipose cells was confirmed by confocal microscopy and/or by fluorescence measurement of isopropyl alcohol extracted lipids. Prior to efflux incubations, cells were washed three times with KRH medium without glucose, BSA, or adenosine, and then 50 µl cells

were added to 500 µl medium (as previously described), containing the cholesterol acceptors. After incubation at 37°C for the indicated times, medium was carefully collected from underneath the cells, and cholesterol efflux quantified by measuring fluorescence (extinction/emission 482 nm/510 nm), in triplicate, using a Victor (Wallac) plate reader.

ApoA-I labeling in adipose cells for immunofluorescence microscopy

ApoA-I Milano or WT were conjugated to ATTO-565 *N*-hydroxysuccinimide-ester (Atto-tech, Siegen, Germany) according to the manufacturer's instructions. In the experiment, ATTO-565-conjugated ApoA-I was used at 10 µg/ml, and nonfluorescent ApoA-I (WT and Milano) was used at 140 µg/ml, making the total ApoA-I concentration 150 µg/ml. Primary rat adipose cells were pretreated with or without glybenclamide (250 µM) for 30 min at 37°C. ApoA-I, WT or Milano (ATTO-565 conjugated and nonfluorescent), was added in the concentrations described above and incubated for 30 min at 37°C. Cells were washed two times with KRH buffer without BSA, followed by fixation in 4% paraformaldehyde for 6 min, washed two times in PBS, blocked, and permeabilized in KRH buffer with 0.1% saponin for 30 min. Primary mouse ABCA1 antibody at a concentration of 2 µg/ml was added and incubated for 1 h. After washing, cells were resuspended in buffer containing Alexa Fluor 488 goat anti-mouse IgG secondary antibody (Alexa Fluor, Molecular Probes, Life Technologies). All steps during cell preparation were performed at room temperature.

TIRF imaging and image analysis

Imaging was performed using a Nikon Ti-E eclipse microscope with a 100× Apo Total internal reflection fluorescence (TIRF) differential interference contrast oil immersion objective with an NA of 1.49 (Nikon Instruments Inc.), an iXon Ultra DU-897 EMCCD camera (Andor Technology Ltd.), and 488 and 561 laser lines (Melles Griot Inc. and Coherent Inc.) with matching filter sets. A TIRF angle corresponding to a TIRF-zone depth of ∼63 nm into the specimen was used during imaging. All images were identically subjected to both background subtraction and threshold settings. Mean intensity values were calculated for region of interest, covering the total membrane surface of the cells in TIRF zone, using NIS Elements, version 4.30.02 (Laboratory Imaging). For each experiment, ∼30 cells/condition/experiment were analyzed.

Statistical analysis

All data are displayed as mean ± SEM. Analysis was performed by Student's *t*-test and two-way ANOVA (**Fig. 1A**) using GraphPad Prism 6 (GraphPad Software Inc.) software. Significance was determined according to the following: * $P \leq 0.05$, ** $P \leq 0.01$, *** $P \leq 0.005$, and **** $P \leq 0.0001$.

RESULTS

ApoA-I Milano treatment induces rapid weight loss and increased lipolysis

Previous studies have reported an association between increased HDL levels and decreased body weight (3–5), and therefore, we wanted to investigate the effect of repeated injections of ApoA-I protein on body weight and composition in an insulin-resistant animal model. Animals were fed an HFD for 2 weeks, followed by one intraperitoneal injection/day of either ApoA-I WT, ApoA-I Milano (20 mg/kg), or saline (NaCl), for 6 days. Twenty-four hours following the first injection, both ApoA-I WT- and Milano-treated mice demonstrated a rapid reduction in body weight (Fig. 1A). After repeated injections, ApoA-I Milano-treated mice displayed a significant reduced body weight throughout the entire treatment period, both compared with ApoA-I WT- and saline-treated animals (Fig. 1A). There were no significant changes comparing ApoA-I WT- and saline-treated mice over the entire time period. Animals treated with Milano, but not WT, displayed a significantly decreased body fat mass as determined by DEXA scan (Fig. 1B). Serum analysis of fed animals showed no changes in NEFA, glucose, or insulin levels (Fig. 1C–E) comparing Milano-, WT-, or saline-treated animals. To examine if the ApoA-I treatment had affected the rate of lipolysis in adipose cells, we isolated primary adipose cells 24 h after the last injection and measured glycerol release into medium. Interestingly, cells isolated from both ApoA-I WT- and Milano-treated mice displayed increased lipolysis compared with cells isolated from saline-treated animals, both nonstimulated and in vitro stimulated with a β-adrenergic receptor agonist (isoproterenol, 10 nM) (Fig. 1F). Western blot analysis of epididymal adipose tissue excised 24 h after the last treatment showed that the injected ApoA-I protein was present in adipose tissue (Fig. 1G). However, no consistent changes in HSL expression level or activation (HSL pS563) were detected (Fig. 1G). Interestingly, protein levels of both caveolin-1 and caveolin-2, known to be involved in intracellular cholesterol trafficking (34), were upregulated in adipose tissue from ApoA-I-treated mice (Fig. 1G).

To examine if the ApoA-I protein itself or the repeated injections caused an immunologic response that could contribute to the reduced body weight, we analyzed blood and serum collected the day after the last treatment. Whole blood analysis showed that the number of WBCs and lymphocytes were unchanged when comparing Milano-, WT-, and saline-injected animals (Fig. 1H). Further, we detected no changes of either TNF-α, IL-6, or IFN-γ levels (Fig. 1I). The animals did not display any signs of immunologic response (i.e., hunching or reluctance to move).

To investigate if reduced food intake contributed to decreased body weight gain, food consumption was measured in a separate study in which daily injections were made for 2 days. For comparison, groups of mice received either ApoA-I WT (20 mg/kg), Milano (20 mg/kg), BSA (20 mg/kg), or NaCl. ApoA-I treatment reduced food intake, and this effect was more pronounced following Milano treatment, compared with ApoA-I WT, even though the animals received the same dose of ApoA-I protein (Fig. 1J). Because the main weight loss of ApoA-I-treated animals occurred after the first injection (Fig. 1A), a separate serum analysis was made at this time point. TNF-α and IL-6 levels analyzed in serum collected from NaCl, BSA-, ApoA-I WT- or Milano-injected animals were below the detection limit ($\leq$10 pg/ml), whereas the positive control (10 µg lipopolysaccharide for 90 min) showed markedly elevated levels of TNF-α and IL-6 (Fig. 1K).
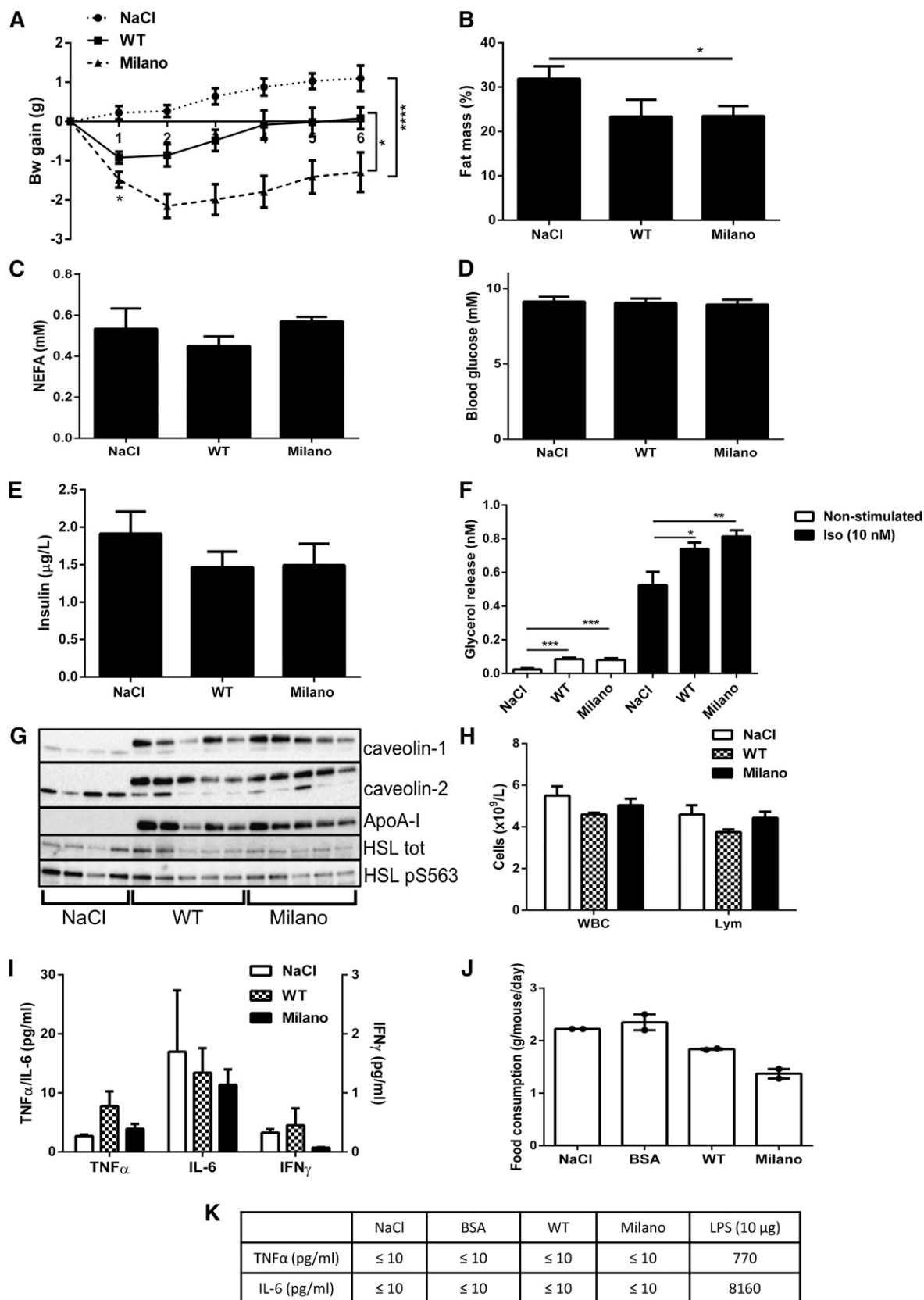
Fig. 1. ApoA-I Milano treatment induces rapid weight loss and increased lipolysis. C57bl6/J mice received one intraperitoneal injection/ day of ApoA-I Milano (20 mg/kg), WT (20 mg/kg), or saline (NaCl), during 6 days (n = 6–11 animals/group). Body weight was monitored daily during the treatment and 24 h after the last injection (day 0 first injection, day 5 last injection) (A). Data presented in B–I were collected 24 h after the last treatment (n = 6–11 animals/group); fat mass determined by DEXA body scan (% body fat mass) (B), serum NEFA (mM) (C), blood glucose (mM) (D), and serum insulin (µg/l) (E). Adipose cells were isolated from epididymal fat tissue, and lipolysis was measured by analyzing glycerol release into medium, either nonstimulated or isoproterenol stimulated (10 nM, 30 min). (F). Adipose tissue

In summary, injections of Milano led to an initial rapid weight loss, leading to a significantly reduced body weight after repeated treatments compared with WT-treated mice. The fact that all ApoA-I-treated mice displayed reduced body weight could in part be explained by decreased food intake. These findings are in line with previous reports in which increased ApoA-I WT expression/levels were associated with decreased body weight and fat mass, and the fact that human carriers of the Milano variant have a favorable metabolic profile. Because the cytokine profile, WBCs, and lymphocytes were unaltered, it is unlikely that these effects were caused by an inflammatory response that otherwise potentially could contribute to an increased lipolytic activity (35). Rather, our interpretation is that the rapid weight loss is due to increased circulating ApoA-1 levels, which affect peripheral tissues as well as food intake.

ApoA-I Milano induces lipolysis in vitro independently of HSL and perilipin phosphorylation

Our finding of increased lipolysis in adipose cells from ApoA-I-treated mice (Fig. 1F) could be due to systemic factors other than ApoA-I. Because earlier studies in vitro have shown that adrenergically stimulated lipolysis could induce cholesterol efflux (20, 21), we wanted to examine if ApoA-I affected nonstimulated lipolysis using an in vitro primary rat adipose cell model. Interestingly, we found that 30 min incubation with either ApoA-I WT or Milano protein (both nonlipidated) stimulated lipolysis in the absence of β-adrenergic stimulation (**Fig. 2A**). Surprisingly, Milano induced a significantly higher glycerol release compared with WT at the same concentration. As a positive control, cells were incubated with isoproterenol (Fig. 2A). In separate experiments, we tested and verified that the Milano-induced glycerol release was dose dependent, shown in Fig. 2B. These results suggest that both ApoA-I WT and the Milano variant exert adipose cell-specific effects leading to increased lipolysis, and that Milano is much more effective at the same concentration.

To explore the signaling pathways involved in mediating ApoA-I-stimulated lipolysis, we performed Western blot analysis of adipose cell lysates generated after incubation. As was expected, β-adrenergic stimulation resulted in phosphorylation of both perilipin (pSer522) and HSL (pSer563), shown in Fig. 2C. However, in line with the data obtained in vivo (Fig. 1G), we detected no ApoA-I WT- or Milano-induced phosphorylation of either perilipin pSer522 or HSL pSer563 (Fig. 2C). Further, ApoA-I did not alter the level of HSL pSer565, a suggested AMP-activated protein kinase site

thought to counteract the activating PKA phosphorylations (Fig. 2C). Preincubation with propranolol, a β-adrenergic receptor antagonist, abolished isoproterenol-induced HSL pSer563 and perilipin pSer522 activation but had no effect in either WT- or Milano-stimulated cells (Fig. 2C). Also, preincubation with propranolol inhibited isoproterenol-induced glycerol release but had no effect on the Milano-stimulated release (supplementary Fig. 1). Western blot analysis showed that isoproterenol, but not Milano, triggered the cAMP/PKA pathway, as detected by phospho-PKA substrate antibody, as well as phosphorylation of the known PKA substrate SIK2 (pSer358) (supplementary Fig. 2) (25). Also, the level of adipose triglyceride lipase expression was unchanged in both ApoA-I Milano- and isoproterenol-treated cells compared with control cells (supplementary Fig. 2) (36).

Because the glycerol assay measures the accumulated glycerol release during 30 min, we also examined shorter time points to investigate if there was a rapid, possibly transient phosphorylation/activation of HSL and perilipin in response to ApoA-I Milano. Already after 5 min of incubation with isoproterenol an increased phosphorylation of perilipin pSer522 and HSL pSer563 was observed (Fig. 2D). However, incubation with Milano for 5 min did not induce the phosphorylation of these targets. Phosphorylation of perilipin pSer522 was further monitored at time points 15 and 30 min without any changes compared with the 5 min time point (Fig. 2D). To investigate the possibility that ApoA-I induced phosphorylation of perilipin on sites other than Ser522, we analyzed perilipin immunoprecipitates using a number of kinase consensus antibodies (14-3-3 binding motif, pPKA-, pPKB-, pPKC-, pCDK-, and pMAPK/CDK substrate). Isoproterenol induced a clear phosphorylation of perilipin on PKA consensus sites, whereas Milano failed to increase the phosphorylation as measured with this or any of the other consensus antibodies (data not shown).

To further test if ApoA-I was dependent on HSL activation, primary adipose cells were preincubated with orlistat, a lipase inhibitor, followed by incubation with either Milano or isoproterenol. The lipase inhibitor reduced the isoproterenol-stimulated lipolysis but had no effect on Milano-stimulated glycerol release (Fig. 2E). In addition to the classical lipolytic pathway, low-grade inflammation (35) and endotoxins (37) have been shown to induce lipolysis through different pathways, both leading to activation of HSL. Our data suggest that ApoA-I-induced lipolysis is independent of HSL activation, and therefore, it is unlikely that the ApoA-I-generated effect is mediated through the inflammatory pathways.

---

was collected and subjected to Western blot analysis to determine caveolin-1, caveolin-2, and HSL protein expression levels; phosphorylation of HSL pS563; and presence of ApoA-I Milano using an ApoA-I-specific antibody (n = 4–5 animals/group) (G). Whole blood was analyzed to determine WBC count and lymphocytes (Lym) ($\times 10^9$/l) (H). Serum collected the day after last treatment was analyzed for levels of TNF-α, IL-6 (left y-axis, pg/ml), and IFN-γ (right y-axis, pg/ml) (I). Food consumption (g/mouse/day) was measured per cage (5 animals/cage). Data displayed as mean from 2 days (J). Serum collected 24 h after the first injection was analyzed for levels of TNF-α and IL-6 (pg/mol); serum from mice treated with 10 μg lipopolysaccharide for 90 min was used as a positive control (n = 5 animals/group) (K). Data in A–K are presented as mean ± SEM. * $P \leqslant 0.05$, ** $P \leqslant 0.01$, *** $P \leqslant 0.0005$, and **** $P \leqslant 0.0001$.
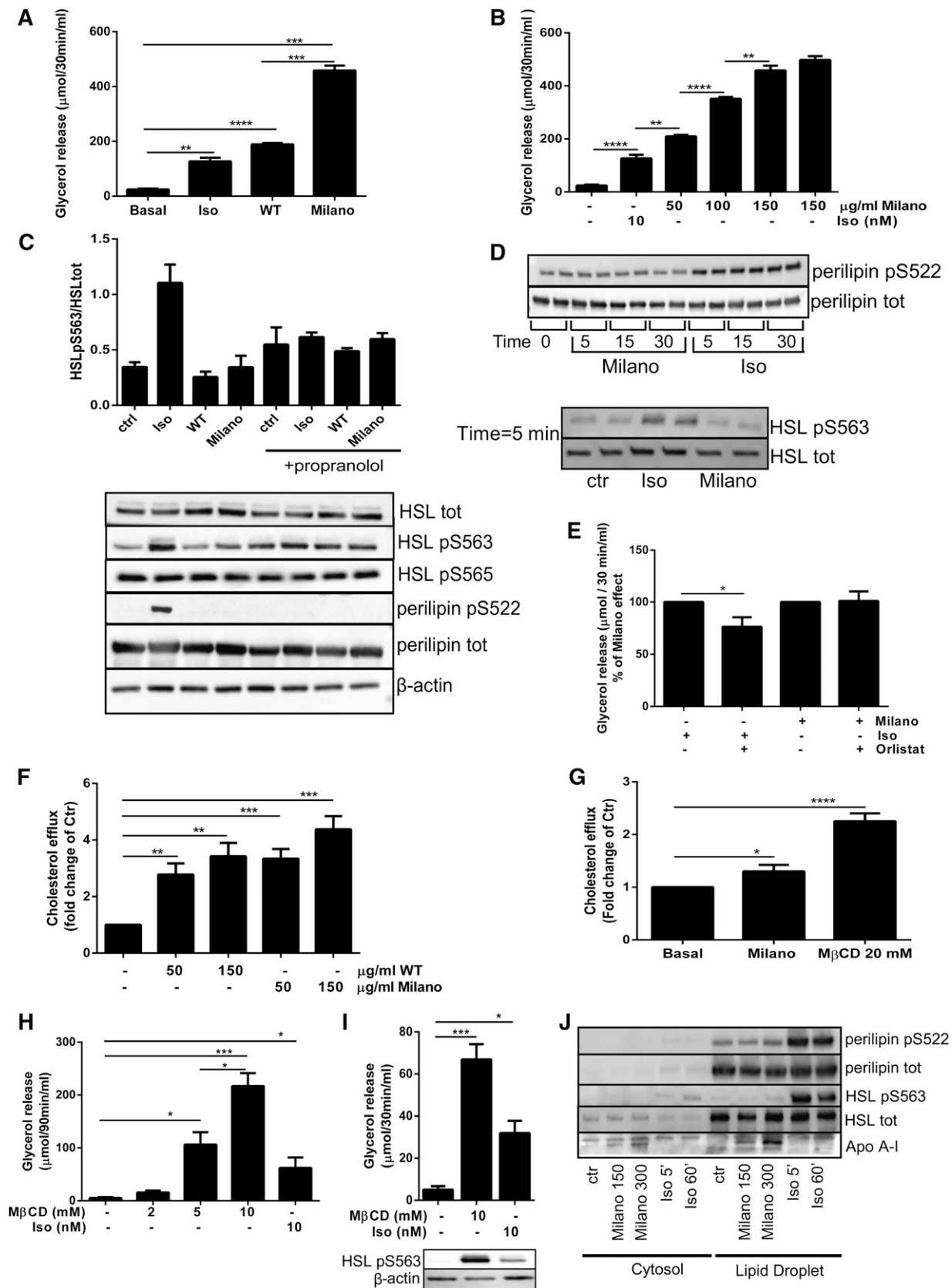
Fig. 2. ApoA-I Milano induces lipolysis in vitro independently of HSL and perilipin phosphorylation. Primary adipose cells were incubated with either Milano (150 µg/ml), WT (150 µg/ml), or isoproterenol (Iso; 10 nM) or left untreated (Basal) for 30 min. Glycerol release was measured in medium (A). Adipose cells were either incubated with lipid-free Milano protein (50–150 µg/ml) or left untreated for 30 min. Glycerol release was measured in medium (B). Data in A and B are presented as µmol/30 min/ml, n = 3 independent experiments, samples run in duplicate. Primary adipose cells were preincubated with or without propranolol (10 µM, 30 min), followed by 30 min incubation with either Milano (150 µg/ml), WT (150 µg/ml), or Iso (10 nM). Cells lysates were subjected to Western blot and analyzed to

In summary, the data show that both ApoA-I Milano and WT trigger lipolysis in primary adipose cells without an increase in the classical cAMP/PKA pathway or any apparent phosphorylation/activation of either perilipin or HSL.

ApoA-I Milano triggers cholesterol efflux in adipose cells

To our knowledge, there are no previous reports that ApoA-I/HDL can independently induce lipolysis. Rather, lipolysis has been shown to induce cholesterol efflux (20, 21). In addition, the cellular effects of the Milano variant have been poorly investigated. Because the data presented herein did not involve the common or inflammatory lipolytic pathway, we wanted to test if the ApoA-I Milano variant could stimulate cholesterol efflux using a 3T3-L1 adipose cell model. Cells preloaded with cholesterol were incubated with either WT or Milano (3 h) followed by analysis of cholesterol content in the medium. Both WT and Milano induced a significant cholesterol efflux, shown in Fig. 2F. We also tested the ability of Milano to stimulate cholesterol efflux in primary adipose cells. MβCD (20 mM) was used as a positive control and induced a ∼2-fold increase of cholesterol efflux (Fig. 2G). In line with previous reports using ApoA-I WT or reconstituted HDL particles, we found that Milano induced cholesterol efflux ∼1.4-fold compared with nonstimulated cells (Fig. 2G). This effect was modest but reproducible and in the same range as previously reported using ApoA-I WT in adipose cells (38). The ability of Milano to remove cholesterol could contribute to the mechanism through which it exerts an effect on lipolysis. Indeed, we discovered that MβCD also stimulated lipolysis in a dose-dependent manner (Fig. 2H). Distinct from Milano, however, MβCD stimulated activation of HSL (Fig. 2I). To examine if there was a cellular uptake of Milano, adipose cells were preincubated with either Milano or isoproterenol, followed by subcellular fractionation to obtain a cytosolic and a lipid droplet fraction. Interestingly, we found Milano to be associated with the lipid droplet (Fig. 2J). As a positive control, we detected both HSL and perilipin in the lipid droplet fraction (Fig. 2J).

Together, these data support the hypothesis that cholesterol efflux could initiate lipolysis, even though MβCD-stimulated lipolysis at least partially is mediated through an HSL-dependent pathway. There is a tightly regulated balance of intracellular cholesterol and triglyceride pools within the cell, and removal of cholesterol from the pool associated with the lipid droplet could be sufficient to promote lipolysis without lipase activation.

ApoA-I WT and Milano stimulate glycerol release independently of ABCA1

In order to examine if Milano-stimulated glycerol release was dependent on ABCA1, a receptor known to be involved in cholesterol efflux and formation of HDL particles (39), we used a well-described inhibitor, glybenclamide, which suppresses ABCA1 ATPase activity and thus inhibits cholesterol efflux (40). However, preincubation of rat adipose cells with glybenclamide (250 μM) prior to ApoA-I WT or Milano incubation did not inhibit ApoA-I-stimulated lipolysis (**Fig. 3A**). To verify this finding, we applied siRNA silencing of ABCA1 in differentiated 3T3-L1 cells. The efficiency of ABCA1 knock down was determined at the mRNA level using real-time PCR (Fig. 3B). Next, we compared the effect on glycerol release using both ApoA-I WT and the Milano variant in ABCA1-deficient 3T3-L1 cells. Silencing of ABCA1 did not affect isoproterenol-, ApoA-I WT-, or Milano-induced lipolysis (Fig. 3C). Indeed, similar to our finding in rat adipose cells, both ApoA-I WT and Milano induced glycerol release in 3T3-L1 cells (Fig. 3C). Again, the increase in lipolysis was much greater following Milano stimulation than with the same concentration of ApoA-I WT. To further test if ABCA1 was involved in binding of ApoA-I to the cell surface, primary adipose cells were incubated with fluorescently labeled ApoA-I (either WT or Milano; ApoA-I-ATTO-565). The distribution of ApoA-I-ATTO-565 and ABCA1, using an ABCA1 specific antibody, was analyzed by TIRF microscopy at a zone depth of 63 nm into the cells, thus excluding most of the labeling distributed in the cytosolic compartment. Both ABCA1 and ATTO conjugated

determine total protein expression levels of HSL and perilipin, β-actin, phosphorylation of HSL pSer563, HSL pSer565, and perilipin pSer522. The graph represents quantification of Western blot data (three independent experiments) with representative Western blots shown below (C). Cells were incubated with Iso (10 nM) or Milano (150 μg/ml) for time points indicated in the figure (5–30 min). Cell lysates were prepared and subjected to Western blot and analyzed to determine total protein expression levels of HSL and perilipin, and phosphorylation of HSL pSer563, and perilipin pSer522, samples run in duplicates, n = 3 independent experiments. The figures show representative Western blots. (D) Primary adipose cells were preincubated with or without orlistat (100 μM, 45 min), followed by 30 min incubation with either Milano (150 μg/ml) or Iso (10 nM). Glycerol release was measured in medium (% of Milano), n = 3 independent experiments (E). Differentiated 3T3-L1 cells were preloaded with ^{3}H-cholesterol (3 h) and treated with PBS (control) or ApoA-I WT or Milano (concentrations indicated in the figure, 50–150 μg/ml). Cholesterol efflux was measured into the medium [fold of control (ctr)], n = 4 independent experiments (F). Isolated adipose cells were preloaded with cholesterol (1 h) followed by treatment with either PBS, Milano, or MβCD (20 mM) as a positive control. Cholesterol efflux was measured into the medium (fold of ctr), n = 3–5 independent experiments (G). Adipose cells were treated with MβCD (concentration indicated in figure, 2–10 mM) for 90 or 30 min, followed by glycerol release measurement in the medium, expressed as μmol/90 min/mol in (H) and μmol/30 min/mol (I). Cell lysates of stimulated cells were subjected to Western blot to determine β-actin expression and phosphorylation of HSL pSer563 (I). Adipose cells were left untreated (Ctr) or incubated with Milano (150 or 300 μg/ml) for 60 min or Iso (10 nM, 5 or 60 min), followed by homogenization and subcellular fractionation to provide cytosol and lipid droplet fractions, which were subjected to Western blot to determine distribution of ApoA-I, HSL, perilipin, HSL pSer563, and perilipin pSer522. Representative blots shown in figure, n = 3 independent experiments (J). Data in A–C and E–I presented as mean ± SEM. * $P \leqslant 0.05$, ** $P \leqslant 0.01$, *** $P \leqslant 0.0005$, and **** $P \leqslant 0.0001$.
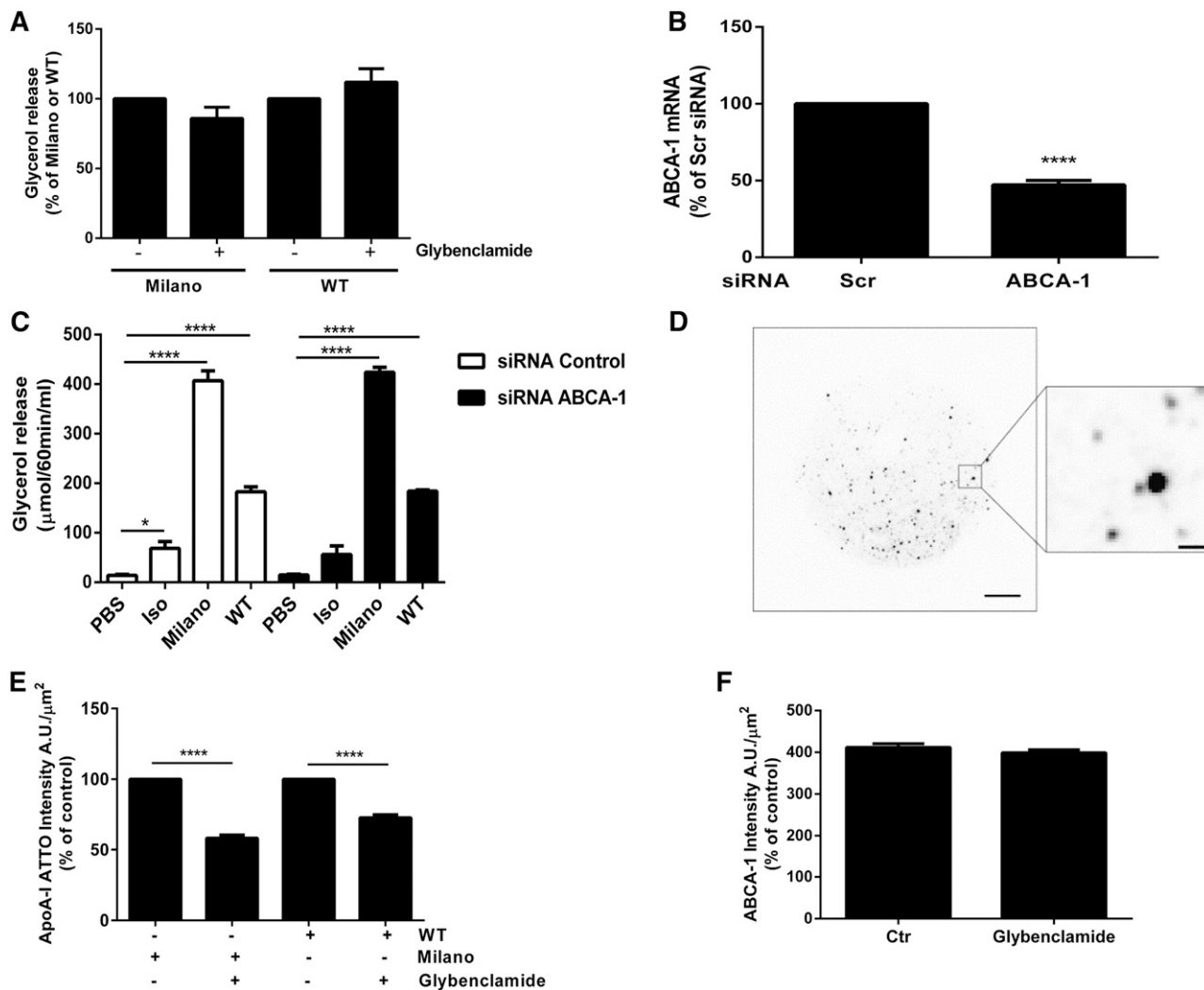
Fig. 3. ApoA-I WT and Milano stimulate glycerol release independently of ABCA1. Rat adipose cells were preincubated with glybenclamide (250 µM) for 30 min, followed by Milano or WT stimulation (150 µg/ml) for an additional 30 min. Lipolysis was determined by measuring glycerol release in the medium. Data are presented as % of Milano or WT, n = 4 independent experiments (A). The expression of ABCA1 was silenced by electroporation of scrambled (scr) or ABCA1 siRNA into differentiated 3T3-L1 cells. ABCA1 expression were determined by real-time PCR analysis (ABCA1 mRNA % of scr), n = 12 (B). Glycerol release was measured in medium from 3T3-L1 cells electroporated with either scr or ABCA1 siRNA, or left untreated (PBS). Data presented as µmol/60 min/ml, n = 3 independent experiments, each condition run in duplicate in each experiment (C). Cells were incubated with fluorescently conjugated Milano-ATTO-565 or WT-ATTO-565 for 30 min (total concentration 150 µg/ml), before fixation and labeling as described in Methods. The distribution of ABCA1 labeling, Milano-ATTO-565, and WT-ATTO-565 was analyzed by TIRF microscopy. A representative image of the ATTO-565 signal captured in the TIRF zone, scale bar = 10 µm, insert scale bar = 1 µm (D). Rat adipose cells were preincubated with glybenclamide (250 µM), before incubation with Milano-ATTO-565 (30 min). Cells were fixed and labeled with ABCA1 antibodies, and the ATTO-565 and ABCA1 signal was detected in separate channels by TIRF microscopy. The graphs in E and F represent quantification of the fluorescence intensity/area unit (A.U./µm^2) of ATTO-565 and ABCA1 labeling detected in the TIRF zone. n = 3–4 independent experiments, image analysis of 30 cells/condition/experiment. Data in A–C, E, and F are presented as mean ± SEM. * $P \leqslant 0.05$, **** $P \leqslant 0.0001$.

with either WT or Milano were found to be distributed as distinct puncta (Fig. 3D). Quantification of the ApoA-I-ATTO-565 signal in the TIRF zone showed that preincubation with glybenclamide (250 µM) significantly reduced the amount of both ApoA-I WT and Milano bound (Fig. 3E). In contrast, the amount of ABCA1 detected at the surface was not altered (Fig. 3F). Together, our data suggest that ABCA1 has the capacity to bind both ApoA-I WT and Milano but is not required for mediating Milano- or ApoA-I WT-induced glycerol release in the two different adipose cell models tested herein.

Caveolae are implicated in different cellular processes such as signal transduction and endocytosis (34, 41), but their specific role in cholesterol efflux is still debated (18, 19). Because almost 50% of the adipose cell surface consists of cholesterol-enriched caveolar membrane, and our in vivo data showed increased caveolin-1 levels in ApoA-I-treated mice (Fig. 1G), we wanted to examine if these structures were required for Milano-induced lipolysis. For this, we made use of adipose cells from caveolin-1-deficient mice, which as a consequence lack caveolae. We found that isoproterenol-stimulated lipolysis was reduced in cells from caveolin-1 KO

mice compared with control cells, which is in agreement with previous findings by Cohen et al (42) (supplementary Fig. 3). However, ApoA-I Milano induced glycerol release to the same extent in cells lacking caveolin-1 compared with control cells. These findings further support the notion that stimulation of adipose cell lipolysis by ApoA-I Milano is independent of classical lipolytic signaling pathways.

DISCUSSION

Apolipoproteins are well known for promoting cholesterol efflux from the vascular wall but have also been shown to promote cholesterol efflux in adipose cell models (43, 44). Considering the limited de novo synthesis of cholesterol in adipose cells, it is reasonable to believe that cholesterol efflux from the adipose cells will affect their function and thus have an impact on whole-body glucose homeostasis (43). Here we wanted to examine the adipose cell-specific effect of Milano, a naturally occurring variant of ApoA-I. Remarkably, we found that treatment of ApoA-I Milano and ApoA-I WT, the latter used as a control throughout the experiments, rapidly induced weight loss in a diet-induced insulin-resistant mouse model. We also found an increased lipolytic activity in adipose cells isolated from the in vivo ApoA-I-treated animals, with no evidence of an elevated systemic inflammatory response, which suggests that ApoA-I exerts a direct effect on adipose cells. This is of great interest because obesity, with altered adipose function, is one of the main risk factors for several metabolic diseases.

Further, we herein report that both ApoA-I WT and the Milano variant promoted cholesterol efflux from adipose cells, which is in line with previous reports using lipid-free ApoA-I WT or ApoA-I-containing HDL (19, 21). We also present novel findings of both ApoA-I WT- and Milano-stimulated glycerol release, independently of β-adrenergic stimulation, in two different adipose cell models. Compared with WT, Milano exerted a markedly stronger effect on lipolysis but not on cholesterol efflux, demonstrating that there could be different mechanisms involved; such alternative mode of action could account for the well-described effect of Milano on vascular wall function (22).

The lack of HSL and perilipin phosphorylation in response to Milano suggests that increased cholesterol efflux from the adipose cell may instead alter the protection of the lipid droplet surface and thus allow increased lipase activity without changes in phosphorylation. Previous studies have described a balance between lipolysis and cholesterol efflux in adipose cells, where β-adrenergic stimulation of lipolysis in 3T3-L1 adipose cells increased cholesterol efflux to HDL (20, 21). However, in the latter study, presence of HDL did not itself initiate efflux of cholesterol from adipose cells. We hypothesize that the cholesterol efflux induced by Milano will alter the cholesterol distribution within the lipid droplet, diminishing the protection against lipolysis. We also observed that Milano was associated with the lipid droplet, and endocytosis of ApoA-I Milano could potentially lead to cholesterol removal not only

at the site of the plasma membrane but also at the intracellular site of cholesterol storage. Indeed, it has been reported that cholesterol efflux from mature human adipose cells is mediated independently of cAMP but is dependent on intact intracellular cholesterol trafficking, thus supporting our data suggesting cholesterol removal from the lipid droplet (45). Also, our finding of a somewhat surprising robust MβCD-induced glycerol release supports the concept of a balance between cholesterol and triglycerides. Previous microscopy analysis revealed that both MβCD and ApoA-I WT promoted redistribution of lipid droplet-associated cholesterol (46). In addition to the classical lipolytic pathway, low-grade inflammation has been suggested to stimulate lipolysis through the inhibitor of nuclear factor κB kinase subunit beta/nuclear factor κB pathway (35), and endotoxins to induce lipolysis through Toll-like receptor 4 (37), both pathways leading to HSL activation. Our data of ApoA-I-mediated lipolysis appear to be independent of HSL activation, and taken together with the lack of a systemic inflammatory response, this suggests the effects of ApoA-I we observed, both in vivo and in vitro, are independent of inflammatory-mediated pathways.

The proposed mechanism underlying the extremely efficient cholesterol removal ability of the Milano variant in humans is based on its altered structural properties, with an additional cysteine bridge favoring dimerization with ApoA-II, another HDL-associated lipoprotein (47). In our in vitro system, the Milano variant was much more potent in triggering lipolysis than ApoA-I WT, and thus, unless adipose cells secrete ApoA-II, the greater effect of Milano versus WT is independent of the structural interaction with ApoA-II. Still, other ApoA-I Milano-specific structural properties could very well account for the increased efficiency in stimulating lipolysis.

ABCA1 is a central component in the early phase of reverse cholesterol transport. Our data suggest that ABCA1 is involved in binding Milano but is not required for mediating ApoA-I WT- or Milano-stimulated lipolysis. Future image analysis could be helpful for verifying the subcellular location of Milano and to explore potential cholesterol redistribution from the lipid droplet that in turn could lead to increased lipolysis. Ultimately, live cell imaging of both lipolysis and cholesterol trafficking could provide useful knowledge about substrate trafficking within the cell, both in the normal and in the obese state. Because ABCA1 inhibition did not reduce Milano-induced lipolysis, alternative pathways are likely to be involved, for example ABCG1 or possibly passive diffusion, even though the concentration of ApoA-I used herein should act via receptor-specific uptake (48).

Caveolin-1-deficient mice lacking caveolae are resistant to diet-induced obesity and have reduced adipose tissue mass and elevated circulating triglycerides and FFA levels. In agreement with our present study, these mice also show a blunted lipolytic response to β-adrenergic receptor stimulation (42, 49, 50), suggesting defects in lipid storage and adipogenesis. In the presence of ApoA-I Milano, we found a similar increase of lipolysis in adipose cells isolated from

WT and caveolin-1-deficient mice. We therefore conclude that the Milano-induced effect was mediated independently of caveolin-1 and caveolae. These data suggest that the increased protein expression of caveolin-1 and caveolin-2 detected in adipose tissue from Milano-treated mice may be secondary to increased cholesterol efflux within the cell.

In conclusion, we have provided evidence that in primary adipose cells, the ApoA-I Milano variant mediates cholesterol efflux and triggers lipolysis independently of β-adrenergic stimuli. ApoA-I WT also stimulated lipolysis, but to a much lesser degree than Milano. These adipose cell-specific effects may contribute to reduced total body fat mass and possibly improve systemic insulin sensitivity, and, at least to some extent, account for the metabolic profile of human ApoA-I Milano variant carriers.▉

REFERENCES

1. Ansell, B. J., M. Navab, S. Hama, N. Kamranpour, G. Fonarow, G. Hough, S. Rahmani, R. Mottahedeh, R. Dave, S. T. Reddy, et al. 2003. Inflammatory/antiinflammatory properties of high-density lipoprotein distinguish patients from control subjects better than high-density lipoprotein cholesterol levels and are favorably affected by simvastatin treatment. *Circulation.* **108:** 2751–2756.
2. Toikka, J. O., M. Ahotupa, J. S. Viikari, H. Niinikoski, M. Taskinen, K. Irjala, J. J. Hartiala, and O. T. Raitakari. 1999. Constantly low HDL-cholesterol concentration relates to endothelial dysfunction and increased in vivo LDL-oxidation in healthy young men. *Atherosclerosis.* **147:** 133–138.
3. Gatti, A., M. Maranghi, S. Bacci, C. Carallo, A. Gnasso, E. Mandosi, M. Fallarino, S. Morano, V. Trischitta, and S. Filetti. 2009. Poor glycemic control is an independent risk factor for low HDL cholesterol in patients with type 2 diabetes. *Diabetes Care.* **32:** 1550–1552.
4. Drexel, H., S. Aczel, T. Marte, W. Benzer, P. Langer, W. Moll, and C. H. Saely. 2005. Is atherosclerosis in diabetes and impaired fasting glucose driven by elevated LDL cholesterol or by decreased HDL cholesterol? *Diabetes Care.* **28:** 101–107.
5. Drew, B. G., S. J. Duffy, M. F. Formosa, A. K. Natoli, D. C. Henstridge, S. A. Penfold, W. G. Thomas, N. Mukhamedova, B. de Courten, J. M. Forbes, et al. 2009. High-density lipoprotein modulates glucose metabolism in patients with type 2 diabetes mellitus. *Circulation.* **119:** 2103–2111.
6. Peterson, S. J., G. Drummond, D. H. Kim, M. Li, A. L. Kruger, S. Ikehara, and N. G. Abraham. 2008. L-4F treatment reduces adiposity, increases adiponectin levels, and improves insulin sensitivity in obese mice. *J. Lipid Res.* **49:** 1658–1669.
7. Ruan, X., Z. Li, Y. Zhang, L. Yang, Y. Pan, Z. Wang, G. S. Feng, and Y. Chen. 2011. Apolipoprotein A-I possesses an anti-obesity effect associated with increase of energy expenditure and up-regulation of UCP1 in brown fat. *J. Cell. Mol. Med.* **15:** 763–772.
8. Ferreira, S. R., and B. Almeida-Pittito; Japanese-Brazilian Diabetes Study Group. 2009. [Reflection about Japanese immigration to Brazil under the light of body adiposity]. *Arq. Bras. Endocrinol. Metabol.* **53:** 175–182. Portuguese.
9. Han, R., R. Lai, Q. Ding, Z. Wang, X. Luo, Y. Zhang, G. Cui, J. He, W. Liu, and Y. Chen. 2007. Apolipoprotein A-I stimulates AMP-activated protein kinase and improves glucose metabolism. *Diabetologia.* **50:** 1960–1968.
10. Kovanen, P. T., E. A. Nikkila, and T. A. Miettinen. 1975. Regulation of cholesterol synthesis and storage in fat cells. *J. Lipid Res.* **16:** 211–223.
11. Le Lay, S., S. Krief, C. Farnier, I. Lefrere, X. Le Liepvre, R. Bazin, P. Ferre, and I. Dugail. 2001. Cholesterol, a cell size-dependent signal that regulates glucose metabolism and gene expression in adipocytes. *J. Biol. Chem.* **276:** 16904–16910.
12. Balkau, B., J. E. Deanfield, J. P. Despres, J. P. Bassand, K. A. Fox, S. C. Smith, Jr., P. Barter, C. E. Tan, L. Van Gaal, H. U. Wittchen, et al. 2007. International Day for the Evaluation of Abdominal Obesity (IDEA): a study of waist circumference, cardiovascular disease, and diabetes mellitus in 168,000 primary care patients in 63 countries. *Circulation.* **116:** 1942–1951.
13. Kuniyasu, A., S. Hayashi, and H. Nakayama. 2002. Adipocytes recognize and degrade oxidized low density lipoprotein through CD36. *Biochem. Biophys. Res. Commun.* **295:** 319–323.
14. Yvan-Charvet, L., A. Bobard, P. Bossard, F. Massiera, X. Rousset, G. Ailhaud, M. Teboul, P. Ferre, G. Dagher, and A. Quignard-Boulange. 2007. In vivo evidence for a role of adipose tissue SR-BI in the nutritional and hormonal regulation of adiposity and cholesterol homeostasis. *Arterioscler. Thromb. Vasc. Biol.* **27:** 1340–1345.
15. Vassiliou, G., and R. McPherson. 2004. A novel efflux-recapture process underlies the mechanism of high-density lipoprotein cholesteryl ester-selective uptake mediated by the low-density lipoprotein receptor-related protein. *Arterioscler. Thromb. Vasc. Biol.* **24:** 1669–1675.
16. Zhao, S. P., B. L. Yu, X. Z. Xie, S. Z. Dong, and J. Dong. 2008. Dual effects of oxidized low-density lipoprotein on LXR-ABCA1-apoA-I pathway in 3T3–L1 cells. *Int. J. Cardiol.* **128:** 42–47.
17. Velamakanni, S., S. L. Wei, T. Janvilisri, and H. W. van Veen. 2007. ABCG transporters: structure, substrate specificities and physiological roles: a brief overview. *J. Bioenerg. Biomembr.* **39:** 465–471.
18. Le Lay, S., M. Rodriguez, W. Jessup, C. Rentero, Q. Li, S. Cartland, T. Grewal, and K. Gaus. 2011. Caveolin-1-mediated apolipoprotein A-I membrane binding sites are not required for cholesterol efflux. *PLoS One.* **6:** e23353.
19. Sviridov, D., N. Fidge, G. Beaumier-Gallon, and C. Fielding. 2001. Apolipoprotein A-I stimulates the transport of intracellular cholesterol to cell-surface cholesterol-rich domains (caveolae). *Biochem. J.* **358:** 79–86.
20. Wei, H., M. M. Averill, T. S. McMillen, F. Dastvan, P. Mitra, S. Subramanian, C. Tang, A. Chait, and R. C. Leboeuf. 2014. Modulation of adipose tissue lipolysis and body weight by high-density lipoproteins in mice. *Nutr. Diabetes.* **4:** e108.
21. Verghese, P. B., E. L. Arrese, and J. L. Soulages. 2007. Stimulation of lipolysis enhances the rate of cholesterol efflux to HDL in adipocytes. *Mol. Cell. Biochem.* **302:** 241–248.
22. Franceschini, G., C. R. Sirtori, A. Capurso II, K. H. Weisgraber, and R. W. Mahley. 1980. A-IMilano apoprotein. Decreased high density lipoprotein cholesterol levels with significant lipoprotein modifications and without clinical atherosclerosis in an Italian family. *J. Clin. Invest.* **66:** 892–900.
23. Ibanez, B., C. Giannarelli, G. Cimmino, C. G. Santos-Gallego, M. Alique, A. Pinero, G. Vilahur, V. Fuster, L. Badimon, and J. J. Badimon. 2012. Recombinant HDL(Milano) exerts greater anti-inflammatory and plaque stabilizing properties than HDL(wild-type). *Atherosclerosis.* **220:** 72–77.
24. Stenkula, K. G., M. Lindahl, J. Petrlova, J. Dalla-Riva, O. Goransson, S. W. Cushman, E. Krupinska, H. A. Jones, and J. O. Lagerstedt. 2014. Single injections of apoA-I acutely improve in vivo glucose tolerance in insulin-resistant mice. *Diabetologia.* **57:** 797–800.
25. Henriksson, E., H. A. Jones, K. Patel, M. Peggie, N. Morrice, K. Sakamoto, and O. Goransson. 2012. The AMPK-related kinase SIK2 is regulated by cAMP via phosphorylation at Ser358 in adipocytes. *Biochem. J.* **444:** 503–514.
26. Petrlova, J., T. Duong, M. C. Cochran, A. Axelsson, M. Morgelin, L. M. Roberts, and J. O. Lagerstedt. 2012. The fibrillogenic L178H variant of apolipoprotein A-I forms helical fibrils. *J. Lipid Res.* **53:** 390–398.
27. Petrlova, J., J. Dalla-Riva, M. Morgelin, M. Lindahl, E. Krupinska, K. G. Stenkula, J. C. Voss, and J. O. Lagerstedt. 2014. Secondary structure changes in ApoA-I Milano (R173C) are not accompanied by a decrease in protein stability or solubility. *PLoS One.* **9:** e96150.
28. Deronic, A., S. Helmersson, T. Leanderson, and F. Ivars. 2014. The quinoline-3-carboxamide paquinimod (ABR-215757) reduces leukocyte recruitment during sterile inflammation: leukocyte- and context-specific effects. *Int. Immunopharmacol.* **18:** 290–297.
29. Rodbell, M., R. O. Scow, and S. S. Chernick. 1964. Removal and metabolism of triglycerides by perfused liver. *J. Biol. Chem.* **239:** 385–391.
30. Clifford, G. M., C. Londos, F. B. Kraemer, R. G. Vernon, and S. J. Yeaman. 2000. Translocation of hormone-sensitive lipase and

perilipin upon lipolytic stimulation of rat adipocytes. *J. Biol. Chem.* **275:** 5011–5015.

31. Zmuda-Trzebiatowska, E., A. Oknianska, V. Manganiello, and E. Degerman. 2006. Role of PDE3B in insulin-induced glucose uptake, GLUT-4 translocation and lipogenesis in primary rat adipocytes. *Cell. Signal.* **18:** 382–390.

32. Gormand, A., E. Henriksson, K. Strom, T. E. Jensen, K. Sakamoto, and O. Goransson. 2011. Regulation of AMP-activated protein kinase by LKB1 and CaMKK in adipocytes. *J. Cell. Biochem.* **112:** 1364–1375.

33. Sankaranarayanan, S., G. Kellner-Weibel, M. de la Llera-Moya, M. C. Phillips, B. F. Asztalos, R. Bittman, and G. H. Rothblat. 2011. A sensitive assay for ABCA1-mediated cholesterol efflux using BODIPY-cholesterol. *J. Lipid Res.* **52:** 2332–2340.

34. Fielding, C. J., and P. E. Fielding. 2001. Caveolae and intracellular trafficking of cholesterol. *Adv. Drug Deliv. Rev.* **49:** 251–264.

35. Grisouard, J., E. Bouillet, K. Timper, T. Radimerski, K. Dembinski, D. M. Frey, R. Peterli, H. Zulewski, U. Keller, B. Muller, et al. 2012. Both inflammatory and classical lipolytic pathways are involved in lipopolysaccharide-induced lipolysis in human adipocytes. *Innate Immun.* **18:** 25–34.

36. Daval, M., F. Diot-Dupuy, R. Bazin, I. Hainault, B. Viollet, S. Vaulont, E. Hajduch, P. Ferre, and F. Foufelle. 2005. Anti-lipolytic action of AMP-activated protein kinase in rodent adipocytes. *J. Biol. Chem.* **280:** 25250–25257.

37. Zu, L., J. He, H. Jiang, C. Xu, S. Pu, and G. Xu. 2009. Bacterial endotoxin stimulates adipose lipolysis via toll-like receptor 4 and extracellular signal-regulated kinase pathway. *J. Biol. Chem.* **284:** 5915–5926.

38. Le Lay, S., C. Robichon, X. Le Liepvre, G. Dagher, P. Ferre, and I. Dugail. 2003. Regulation of ABCA1 expression and cholesterol efflux during adipose differentiation of 3T3–L1 cells. *J. Lipid Res.* **44:** 1499–1507.

39. Vedhachalam, C., P. T. Duong, M. Nickel, D. Nguyen, P. Dhanasekaran, H. Saito, G. H. Rothblat, S. Lund-Katz, and M. C. Phillips. 2007. Mechanism of ATP-binding cassette transporter A1-mediated cellular lipid efflux to apolipoprotein A-I and formation of high density lipoprotein particles. *J. Biol. Chem.* **282:** 25123–25130.

40. Takahashi, K., Y. Kimura, N. Kioka, M. Matsuo, and K. Ueda. 2006. Purification and ATPase activity of human ABCA1. *J. Biol. Chem.* **281:** 10760–10768.

41. Gustavsson, J., S. Parpal, M. Karlsson, C. Ramsing, H. Thorn, M. Borg, M. Lindroth, K. H. Peterson, K. E. Magnusson, and P. Stralfors. 1999. Localization of the insulin receptor in caveolae of adipocyte plasma membrane. *FASEB J.* **13:** 1961–1971.

42. Cohen, A. W., B. Razani, W. Schubert, T. M. Williams, X. B. Wang, P. Iyengar, D. L. Brasaemle, P. E. Scherer, and M. P. Lisanti. 2004. Role of caveolin-1 in the modulation of lipolysis and lipid droplet formation. *Diabetes.* **53:** 1261–1270.

43. Zhang, Y., F. C. McGillicuddy, C. C. Hinkle, S. O'Neill, J. M. Glick, G. H. Rothblat, and M. P. Reilly. 2010. Adipocyte modulation of high-density lipoprotein cholesterol. *Circulation.* **121:** 1347–1355.

44. Angel, A., R. Yuen, and J. A. Nettleton. 1981. Exchange of free cholesterol between low density lipoproteins and human adipocytes. *Can. J. Biochem.* **59:** 655–661.

45. Bencharif, K., L. Hoareau, R. K. Murumalla, E. Tarnus, F. Tallet, R. G. Clerc, C. Gardes, M. Cesari, and R. Roche. 2010. Effect of apoA-I on cholesterol release and apoE secretion in human mature adipocytes. *Lipids Health Dis.* **9:** 75.

46. Prattes, S., G. Horl, A. Hammer, A. Blaschitz, W. F. Graier, W. Sattler, R. Zechner, and E. Steyrer. 2000. Intracellular distribution and mobilization of unesterified cholesterol in adipocytes: triglyceride droplets are surrounded by cholesterol-rich ER-like surface layer structures. *J. Cell Sci.* **113:** 2977–2989.

47. Zhu, X., G. Wu, W. Zeng, H. Xue, and B. Chen. 2005. Cysteine mutants of human apolipoprotein A-I: a study of secondary structural and functional properties. *J. Lipid Res.* **46:** 1303–1311.

48. von Eckardstein, A., and C. Widmann. 2014. High-density lipoprotein, beta cells, and diabetes. *Cardiovasc. Res.* **103:** 384–394.

49. Martin, S., M. A. Fernandez-Rojo, A. C. Stanley, M. Bastiani, S. Okano, S. J. Nixon, G. Thomas, J. L. Stow, and R. G. Parton. 2012. Caveolin-1 deficiency leads to increased susceptibility to cell death and fibrosis in white adipose tissue: characterization of a lipodystrophic model. *PLoS One.* **7:** e46242.

50. Razani, B., T. P. Combs, X. B. Wang, P. G. Frank, D. S. Park, R. G. Russell, M. Li, B. Tang, L. A. Jelicks, P. E. Scherer, et al. 2002. Caveolin-1-deficient mice are lean, resistant to diet-induced obesity, and show hypertriglyceridemia with adipocyte abnormalities. *J. Biol. Chem.* **277:** 8635–8647.